Soler, N.; Fagoaga García, CC.; López Del Rincón, C.; Moreno, P.; Navarro, L.; Flores Pedauye, R.; Peña Garcia, L. (2015). Symptoms induced by transgenic expression of p23 from Citrus tristeza virus in phloem-associated cells of Mexican lime mimic virus infection without the aberrations accompanying constitutive expression. Molecular Plant Pathology. 16(4):388-399. doi:10.1111/mpp.12188.

Symptoms induced by transgenic expression of p23 from *Citrus tristeza virus* in phloem-associated cells of Mexican lime mimic virus infection and do not include aberrations accompanying constitutive expression.

Nuria Soler, Carmen Fagoaga, Carmelo López, Pedro Moreno, Luis Navarro, Ricardo Flores and Leandro Peña.

Summary

Citrus tristeza virus (CTV) is phloem-restricted in natural citrus hosts. The 23 kDa protein (p23) encoded by the virus is an RNA silencing suppressor and a pathogenicity determinant. Expression of p23, or its N-terminal 157 amino acid fragment comprising the zinc-finger and flanking basic motifs, driven by the constitutive 35S promoter incites CTV-like symptoms and other aberrations in transgenic citrus. To better define the role of p23 in CTV pathogenesis, we compared the phenotypes of Mexican limes transformed with p23-derived transgenes from the severe T36 or the mild T317 CTV strains under the control of the phloem-specific promoter from *Commelina yellow mottle virus* (CoYMV) or the 35S promoter. Expression of the constructs restricted to the phloem incited aberrations resembling CTV-specific symptoms (vein clearing and necrosis, and stem pitting), but not the non-specific symptoms (like mature leaf epinasty and yellow pinpoints, growth cease and apical necrosis) observed when p23 was ectopically expressed. Furthermore, vein necrosis and stem pitting in Mexican lime appeared specifically associated with p23 from T36. Phloem-specific accumulation of the p23Δ158-209(T36) fragment was sufficient to incite the same anomalies, indicating that the region comprising the N-terminal 157 amino acids of p23 is responsible (at least in part) for the vein clearing, stem pitting and possibly vein corking in this host.

3.3.1. Introduction

Citrus tristeza virus (CTV) is the causal agent of devastating epidemics that have changed the course of the citrus industry, provoking the worldwide loss of almost 100 million tress of sweet orange (*Citrus sinensis* (L.) Osb.), mandarin (*C. reticulata* Blanco), grapefruit (*C. paradisi* Macf.) and lime (*C. aurantifolia* (Christ.) Swing.) propagated on sour orange (*C. aurantium* L.) (Moreno et al., 2008). CTV is a member of the genus *Closterovirus*, family *Closteroviridae*, and it only infects naturally phloem-associated tissues of species of the genera *Citrus* and *Fortunella* within the family *Rutaceae*, subfamily *Aurantoideae*. The virus is readily transmitted with infected buds and spread locally by several aphid species in a semi-persistent mode (Bar-Joseph et al., 1989).

CTV has a plus-strand single-stranded genomic (g)RNA of approximately 19.3 kb organized in 12 open reading frames (ORFs), potentially encoding at least 17 protein products, delimited by 5' and 3' untranslated regions (UTRs) (Karasev et al., 1995). The two 5'-proximal ORFs encode components of the replicase complex (Karasev et al., 1995) and are translated directly from the gRNA (Hilf et al., 1995). The 10 ORFs located in the 3' moiety of the gRNA are expressed through a set of 3' co-terminal subgenomic mRNAs (Hilf et al., 1995) encoding proteins p33, p6, p65, p61, p27, p25, p18, p13, p20 and p23 (Karasev et al., 1995; Pappu et al., 1994). The small hydrophobic p6 is proposed to act as a transmembrane anchor, and p25 and p27 are the major and minor coat proteins, respectively.

About 97% of the gRNA is encapsidated by p25 and the 5'-terminal 650 nucleotides by p27 (Febres et al., 1996; Satyanarayana et al., 2004). These two proteins, together with p65 and p61, are required for virus assembly (Satyanarayana et al., 2000). While p33, p13 and p18 are dispensable for systemic infection of some citrus hosts but required for others (Tatineni et al., 2008; Tatineni et al., 2011), p20, a protein accumulating in amorphous inclusion bodies of CTV-infected cells (Gowda et al., 2000), and p23, are indispensable for invasion of all hosts (Tatineni et al., 2008). Additionally, p33 is needed for superinfection exclusion (Folimonova, 2012).

Unique to CTV is p23, with no homologs found in other closteroviruses (Dolja et al., 2006). It is expressed in early stages of cell infection (Navas-Castillo et al., 1997) and accumulates in infected plants at moderate levels compared to other viral proteins (Pappu et al., 1997). Dolja et al. (1994) showed the presence of a cluster of positively-charged amino acids in p23, and López et al. (1998) further characterized this conserved region that has a core with three cysteines and one histidine forming a putative zinc-finger domain. The presence of this domain suggested a regulatory function for p23, a view supported by the finding that p23 binds RNA *in vitro* in a sequence non-specific manner, and that mutations affecting the cysteine and histidine residues increase the dissociation constant of the p23-RNA complex (López et al., 2000). Moreover, p23 is involved in regulating the balance of plus and minus viral strands during replication, with the zinc finger domain and an adjacent basic region being indispensable for asymmetrical accumulation of the plus strand (Satyanarayana et

al., 2002). Together with p20 and p25, p23 acts as an RNA silencing suppressor (RSS) in *Nicotiana tabacum* and *N. benthamiana*, with p25 acting intercellularly, p23 intracellularly, and p20 at both levels (Lu et al., 2004). In addition, p23 is a viral pathogenicity determinant when expressed ectopically in citrus (see below). Moreover, the seedling yellows syndrome, induced by some CTV strains in sour orange and grapefruit, has been mapped at the p23-3′UTR region (Albiach-Martí et al., 2010).

The viral region coding for p23 is a hotspot for RNA silencing because small (s)RNAs from this region accumulate to high levels in CTV-infected Mexican lime and sweet orange (Ruiz-Ruiz et al., 2011). Ectopic expression of p23 enhances systemic infection and virus accumulation in transgenic sour orange and facilitates CTV escaping from the phloem of transgenic sweet and sour orange. Therefore, constraints to CTV movement in some citrus hosts, particularly in sour orange, may at least in part result from RNA silencing (Fagoaga et al., 2011). Moreover, recent data indicate that p23 accumulates preferentially in the nucleolus and Cajal bodies, as well as in plasmodesmata, being some basic motifs and the zinc-finger domain essential for nucleolar localization (Ruiz-Ruiz et al., 2013). The same motifs/domain are sufficient for inducing necrosis in *N. benthamiana* when p23 is expressed from *Potato virus X* and for inciting CTV-like aberrations in transgenic Mexican lime plants, thus linking pathogenicity of p23 to its nucleolar localization. In contrast, most p23 regions are needed for RSS activity in *N. benthamiana* (Ruiz-Ruiz et al., 2013).

The use of transgenic plants has been instrumental in identifying viral RSS and pathogenicity determinants, though most of this work has been restricted to *Nicotiana spp*. and *Arabidopsis thaliana* (Díaz-Pendón and Ding, 2008). However, transgenic expression of RSS in non-natural hosts does not necessarily reflect the effects of viral infection, because in their natural context these proteins are often expressed only in infected cells and tissues, unlike the constitutively expressed transgenes (Csorba et al., 2009; Díaz-Pendón and Ding, 2008). Alternatively, mutant viruses expressing dysfunctional proteins have been used to assess their role as pathogenicity determinants (Hsieh et al., 2009; Yambao et al., 2008; Ziebell and Carr, 2009). Unfortunately, this approach can neither be extended to p23 because it is essential for CTV replication (Satyanarayana et al., 1999), nor be replaced by a homolog from a related virus because p23 is unique among closteroviruses. Symptoms induced by certain CTV strains in citrus, such as vein clearing and stem pitting, are specific of this pathosystem and are recapitulated by some of the aberrations associated with the constitutive expression of p23 in Mexican lime. However, other non-specific symptoms accompanying the constituive expression of p23, like mature leaf epinasty and yellow pinpoints, growth cease and apical necrosis (Fagoaga et al., 2005; Ghorbel et al., 2001), are rarely seen in non-transgenic CTV-infected Mexican lime and other citrus species. These latter aberrations most likely result from the ectopic expression of p23 in cells other than those associated with the phloem, the only tissue infected by CTV.

To better define the role of p23 in CTV pathogenesis, we have now restricted the transgenic expression of p23 to phloem-associated cells of Mexican lime. For this purpose, constructions carrying different versions of p23 or fragments thereof, have been put under the control of the phloem-specific promoter from *Commelina yellow mottle virus* (CoYMV) (Medberry et al., 1992). We show here that: 1) aberrations associated with phloem-specific expression and accumulation of p23 are essentially identical to symptoms caused by CTV infection in Mexican lime, 2) some of these CTV-like symptoms induced by p23 from the severe strain T36 were not observed when using p23 from the mild strain T317, thus mimicking the effects of natural infections by both CTV strains, and 3) similar restricted expression of the fragment comprising the zinc-finger and flanking basic motifs of p23 is sufficient to induce the CTV-like aberrations, confirming that the N-terminal region of 157-amino acids determines, at least in part, CTV pathogenesis in Mexican lime.

3.3.2. Results and discussion

Vein clearing in Mexican lime transformed with CoYMV-*p23* constructs resembles that induced by CTV in non-transformed plants and correlates in intensity with p23 accumulation

Based on transgene integrity of *p23* and on locus/loci patterns, as determined by enzyme restriction and Southern-blot hybridization, at least ten independent Mexican lime lines were generated for each of the three constructs, CoYMV-*p23*(T36), CoYMV-*p23Δ158-209*(T36)

and CoYMV-*p23*(T317), as well as for the empty vector (EV) (Figure 1a). The selected transgenic lines contained at least one intact copy of the CoYMV-driven expression cassette (Figure 1c), and an estimated number of transgene loci ranging between one and four (Figure 1b). Moreover, Northern-blot analysis showed variable transgene expression depending on the line, with an inverse but not strict correlation between transgene loci number and transcript expression being observed (Figure 1d and 1e). Five propagations were prepared from each of the three selected CoYMV-*p23* and EV transgenic lines, as well as from selected 35S-*p23*-transgenic lines of Mexican lime generated and characterized in previous studies (Fagoaga et al., 2005; Ghorbel et al., 2001; Ruiz-Ruiz et al, 2013). CTV-infected non-transformed plants were also propagated in parallel and used as controls.

About 3-6 months after propagation in the greenhouse, transgenic Mexican limes harboring the CoYMV-*p23*(T36), CoYMV-*p23Δ158-209*(T36) or CoYMV-*p23*(T317) cassettes, displayed progressively vein clearing in developing leaves, in contrast with the asymptomatic phenotype exhibited by similar leaves from plants transformed with the EV cassette (Figure 2). This phenotypic anomaly was essentially identical to the vein clearing incited by CTV T36 in non-transgenic plants of this host (Figure 2; C+CTV lanes and corresponding leaf samples).

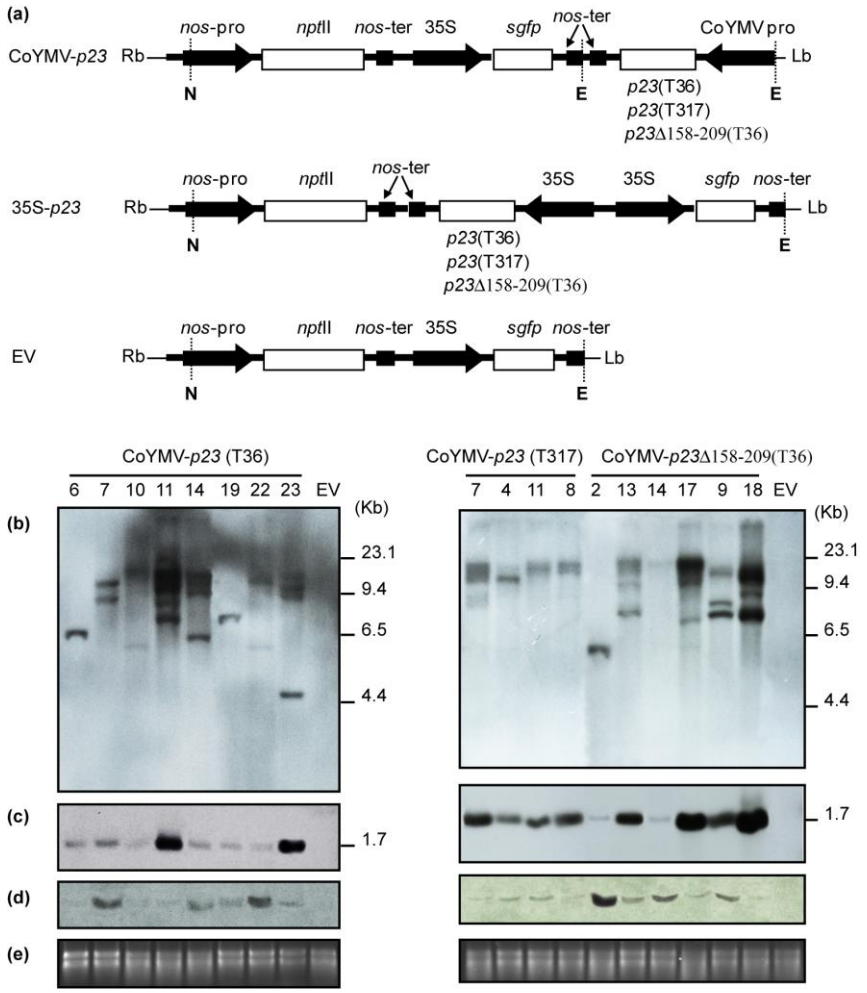

Figure 1 Diagram of the T-DNA from the binary vectors CoYMV-*p23* and 35S-*p23*, and Southern/Northern blot analyses from transgenic Mexican limes. (a) Diagram of the T-DNA from the binary vectors CoYMV-*p23* and 35S-*p23* carrying *p23*(T36), *p23*(T317) or *p23Δ158-209*(T36) cassettes under the control of the phloem-specific promoter from *Commelina yellow mottle virus* (CoYMV-pro) and the *nopaline synthase* terminator (*nos*-ter), and the constitutive 35S promoter from the *Cawliflower mosaic virus* (35S-pro) and the *nos*-ter, respectively. These cassettes were flanked by the *neomycin phosphotransferase* II gene (*npt*II) between the *nos* promoter (*nos*-pro) and *nos*-ter, and by the *green fluorescent protein* gene (s*gfp*) between 35S-pro and *nos*-ter. The binary vector pBin19-s*gfp* was used as empty vector (EV) control. Transcription orientation for each cassette is indicated by arrows. N and E denote *Nhe*I and *Eco*RI restriction sites, respectively. (continued)

Figure 1 (continued) (b, c, d and e) Southern and Northern blot hybridization of nucleic acid preparations from lime plants transformed with the CoYMV-*p23*(T36) construct (lines 6, 7, 10, 11, 14, 19, 22 and 23), the CoYMV-*p23*(T317) construct (lines 7, 4, 11 and 8), the CoYMV-*p23Δ158-209*(T36) construct (lines 2, 13, 14, 17, 9 and 18) and with the empty vector (EV). DNA was digested with *Nhe*I (b), which cuts once the T-DNA, or with *Eco*RI (c), which excises the CoYMV-*p23* expression cassette. Size of DNA markers is indicated at the right. (d) Total RNA extracted from transgenic plants was separated by electrophoresis in a formaldehyde-containing agarose gel, and transferred to a nylon membrane. (e) Ethidium bromide staining of the RNA gel showing that equivalent amounts of RNA were loaded in the different lanes. (b, c, and d) Membranes were probed with a digoxigenin-labeled fragment of the *p23*-coding region.

All CoYMV-*p23* Mexican lime transformants accumulated detectable amounts of p23 or p23Δ158-209, unlike those plants carrying the EV construct, as revealed by Western-blot analysis (Figure 2). Moreover, accumulation of p23 from CTV T36 or T317, or p23Δ158-209 from T36 in CoYMV-*p23*(T36), CoYMV-*p23*(T317) and CoYMV-*p23Δ158-209*(T36) transgenic plants, respectively, correlated positively with the CTV-like vein clearing intensity. For example, lines CoYMV-*p23*(T36)-7 and -22 (Figure 2a), lines CoYMV-*p23*(T317)-8 and -11 (Figure 2b), and lines CoYMV-*p23Δ158-209* (T36)-2 and -9 (Figure 2c), displayed pronounced vein clearing and high p23 accumulation, while lines CoYMV-*p23*(T36)-23 and -6 (Figure 2a), lines CoYMV-*p23*(T317)-4 and -7 (Figure 2b) and lines CoYMV-*p23Δ158-209*(T36)-14 and -17 (Figure 2c) showed milder vein clearing and accumulated low to moderate levels of p23 (Figure 2). Therefore, the phloem-specific expression of p23 from the mild strain T317 induced in Mexican lime vein clearing similar to that incited by the severe strain T36, with the intensity being correlated with p23 accumulation irrespective of the source strain, as previously reported for the constitutive expression of p23 from both strains (Fagoaga et al., 2005).

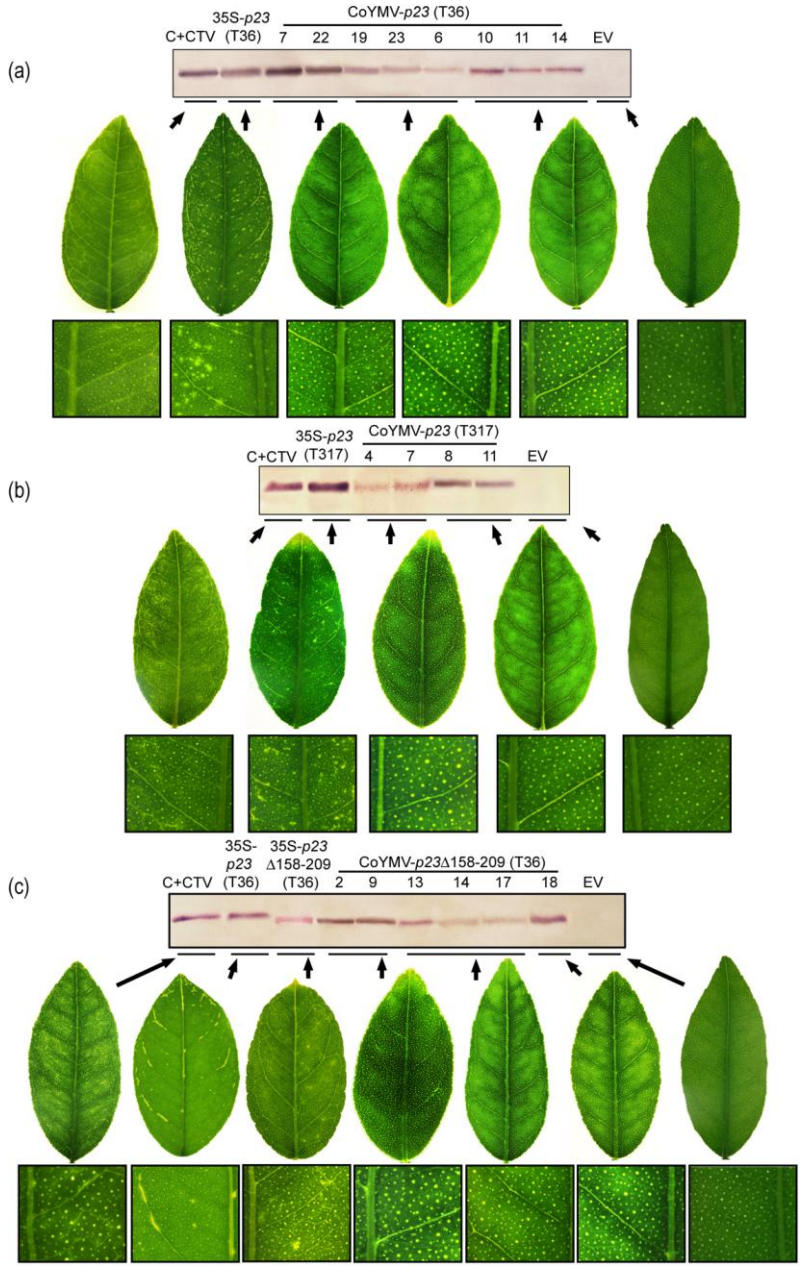

Figure 2 Accumulation of the p23 protein and vein clearing symptoms in developing leaves from transgenic Mexican limes. Western-blot analysis of protein preparations separated by SDS-PAGE (12%) and probed with a specific antibody of: (a) p23 from CTV T36, (b) p23 from CTV T317, and (c) p23Δ158-209 from CTV T36. Vein clearing shown by leaves of Mexican lime transformed with: (a) CoYMV-*p23*(T36), (b) CoYMV-*p23*(T317), and (c) CoYMV-*p23Δ158-209*(T36), Controls include non-transgenic Mexican limes infected with CTV T36 (C+CTV), and 35S-*p23* and empty vector (EV) transgenic plants. To better illustrate vein clearing, a magnification is shown below each leaf.

Mexican lime transformed with CoYMV-*p23* constructs develops stem pitting and vein necrosis similar to those induced by the severe CTV strain T36 in non-transformed plants

Six to twelve months after being propagated in the greenhouse, transgenic plants CoYMV-*p23*(T36) and CoYMV-*p23Δ158-209*(T36) exhibited stem pitting similar to that of transgenic plants 35S-*p23*(T36) (Ghorbel et al., 2001) and 35S-*p23Δ158-209*(T36) (Ruiz-Ruiz et al., 2013) (Figure 3a). This phenotypic aberration was also very similar to the stem pitting induced by CTV T36 in non-transgenic Mexican lime, though pitting was more pronounced and extended in this latter case (Figure 3a). The stem pitting intensity was comparable in all transgenic plants expressing the different versions of p23 and p23Δ158-209, irrespective of their accumulation levels (data not shown). This lack of correlation is possibly associated with weak stem pitting incited by both p23(T36) versions in transgenic Mexican limes (Figure 3a). Conversely, CoYMV-*p23*(T317) transgenic plants accumulating p23 did not show stem pitting at any developmental stage, behaving as the EV transgenic controls (Figure 3a). As 35S-*p23*(T317) transgenic plants neither displayed stem pitting (Figure 3a; Fagoaga et al., 2005), our results indicate that this symptom is depends on the p23 source rather than on its accumulation level. In non-transformed Mexican lime, strain T317 causes only mild vein clearing (Moreno et al., 1993).

After one year in the greenhouse, transgenic plants CoYMV-*p23*(T36) and CoYMV-*p23Δ158-209*(T36) exhibited vein necrosis in

the lower surface of mature leaves, resembling vein corking incited in non-transformed Mexican lime by severe CTV strains, including T36, though such vein corking usually occurs in the upper leaf surface (Figure 3b). Moreover, the intensity of vein necrosis paralleled generally accumulation of p23. For example, while lines CoYMV-*p23*(T36)-7 and -11 and lines CoYMV-*p23Δ158-209*(T36)-2 and -9 displayed marked vein necrosis and accumulated high to moderate levels of p23, lines CoYMV-*p23*(T36)-6 and -23 and lines CoYMV-*p23Δ158-209*(T36)-14 and -17 showed mild vein necrosis and lower p23 accumulation (Figure 2a and c; Figure 3b; data not shown). In contrast, vein necrosis was absent in transgenic plants CoYMV-*p23*(T317), as well as in transgenic plants 35S-*p23*(T36), 35S-*p23Δ158-209*(T36), 35S-*p23*(T317) and EV (Figure 3b), indicating that this aberration is exclusively associated to phloem-specific expression of p23 from T36. Therefore, the most severe phenotypic effects in Mexican lime transformants (stem pitting and vein necrosis) seem related to the source of p23 and, more specifically, to its N-terminal fragment of 157 amino acids.

Comparison of the predicted amino acid sequence of p23 from 18 CTV isolates of different pathogenicity showed three regions (demarcated by positions 24-29, 50-54 and 78-80), in which mild CTV isolates, but not other isolates, have the same sequence (Sambade et al., 2003). Interestingly, these regions include most amino acid differences between p23 from T317 and T36 (or its Δ158-209 version).

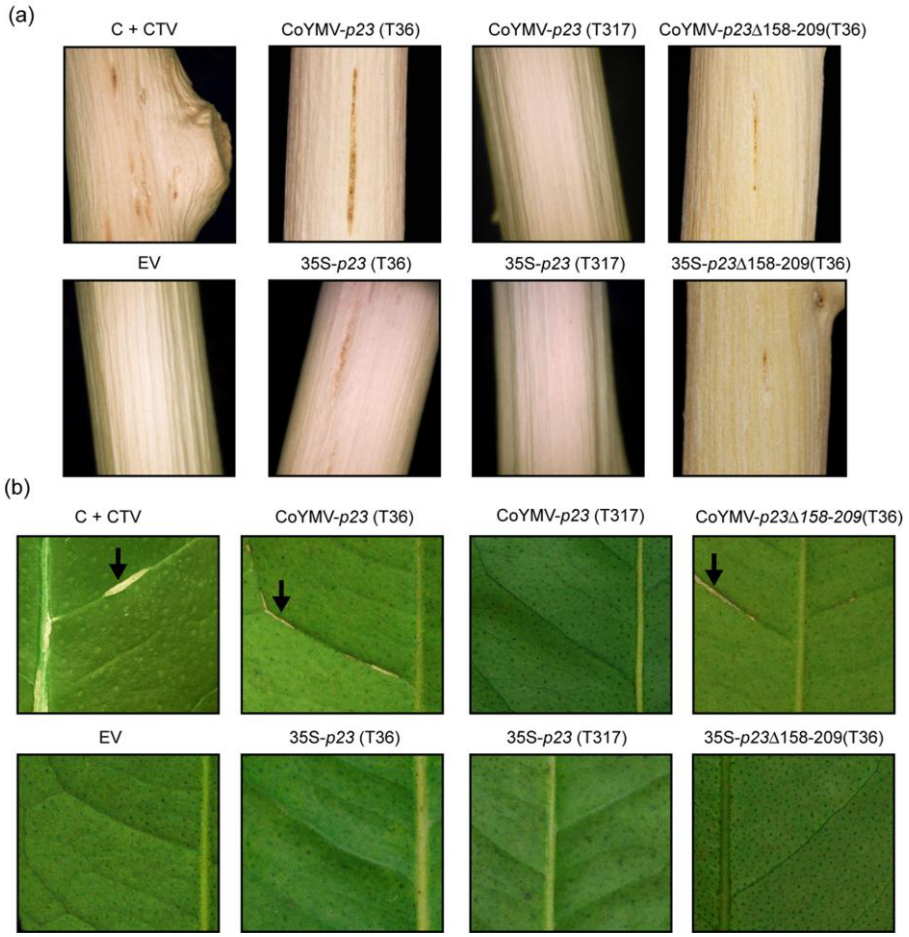

Figure 3 Stem pitting and vein necrosis CTV-like symptoms exhibited by CoYMV-*p23*(T36)- and CoYMV-*p23Δ158-209*(T36)-transgenic Mexican limes. Stem pitting (a) and vein necrosis (b) CTV-like symptoms exhibited by CoYMV-*p23*(T36)- and CoYMV-*p23Δ158-209*(T36)-transgenic Mexican limes. Neither stem pitting nor vein necrosis was detected in CoYMV-*p23*(T317)-transgenic plants (a, b). Controls include non-transgenic Mexican limes inoculated with CTV T36 (C+CTV), and 35S-*p23*(T36)-, 35S-*p23Δ158-209*(T36)- and 35S-*p23*(T317)- and EV-transgenic plants.

Regions 50-54 and 78-80 form part of two domains that include several basic residues (positions 50-67) and a putative zinc finger motif (positions 68-86), which are crucial for the RNA-binding

activity of p23 (López et al., 1998) and for its nucleolar localization (Ruiz-Ruiz et al., 2013). Altogether these results support the involvement of the p23 fragment encompassing the N-terminal 157 amino acids in the induction of the CTV-like stem pitting and vein necrosis.

Aberrations induced by phloem-specific expression of p23 or its N-terminal fragment of 157 amino acids in Mexican lime are histologically similar to those incited by CTV in non-transformed plants

To corroborate that vein clearing induced by the phloem-specific expression of p23 from T317, and vein clearing and necrosis induced by the phloem-specific expression of p23 and p23Δ158-209 from CTV T36 in Mexican lime mimic symptoms incited by the corresponding CTV strain in non-transformed plants, we looked at cross sections of leaf veins from: i) transgenic plants CoYMV-*p23*(T36), CoYMV-*p23*(T317) and CoYMV-*p23Δ158-209*(T36), ii) transgenic plants 35S-*p23*(T36), 35S-*p23*(T317), 35S-*p23Δ158-209*(T36) and EV, and iii) non-transformed controls infected with CTV T36 (C+CTV).

Examination by light microscopy showed that the xylem cap, phloem, and phloem fibers were fully differentiated in EV control veins, with air spaces on each side of the vein (Figure 4a, i). However, vein clearing areas in CTV-infected plants (C+CTV) showed hypertrophied cells developed from the primary phloem fibers, which

occluded air spaces found normally around veins (Figure 4b). Differentiation failed to occur, so veins lacked the caps of primary phloem fibers and sheath cells (Schneider, 1959). Vein clearing areas from CoYMV-*p23*(T36), CoYMV-*p23*(T317), CoYMV-*p23Δ158-209*(T36) (Figure 4f, 4g and 4h, respectively) and 35S-*p23*(T36), 35S-*p23*(T317), 35S-*p23Δ158-209*(T36) (Figure 4c, 4d and 4e, respectively) leaves displayed obliterated cells in the phloem cap and hypertrophied cells occluding part of the air spaces found normally around veins. Therefore, vein clearing shown by CoYMV-*p23* plants was histologically undistinguishable from that exhibited by 35S-*p23* plants and similar to, albeit less intense than, vein clearing incited by CTV T36 in the non-transformed counterparts. Cross sections from necrotic veins in CoYMV-*p23*(T36) (Figure 4k) and CoYMV-*p23Δ158-209*(T36) plants (Figure 4l) displayed excessive phloem formation displacing phloem fibers, and the phloem cap showed obliterated cells as well as collapsed and necrotic areas. Corking areas from C+CTV leaves exhibited a disorganized tissue, also with phloem overformation, obliterated cells, collapsed and necrotic areas, and lack of phloem fibers (Figure 4j). These results indicate that vein necrosis in CoYMV-*p23*(T36) and CoYMV-*p23Δ158-209*(T36) transgenic limes strongly resembles vein corking incited by CTV in this host, but with more pronounced tissue disorganization and necrosis in the second case (Figure 4j, k, l).

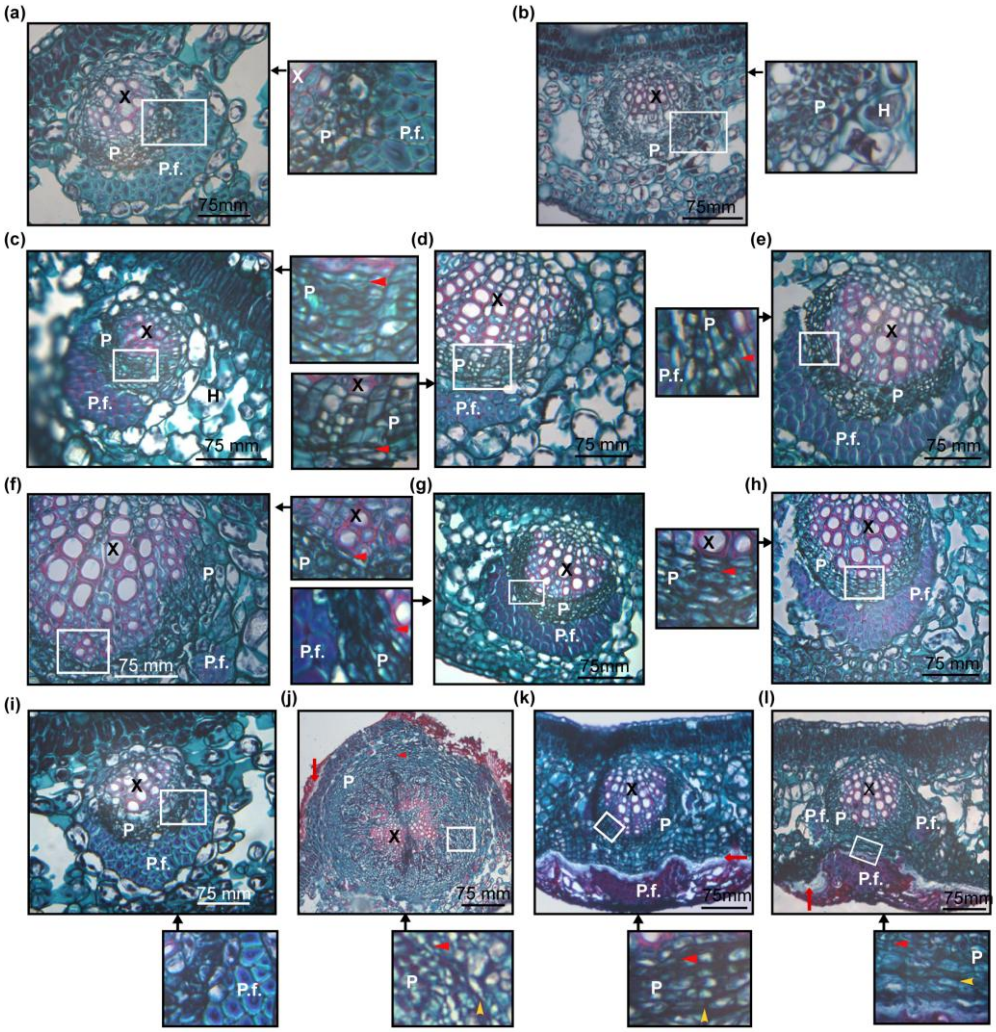

Figure 4 Cross sections of representative leaf veins from CoYMV-*p23*(T36)-, CoYMV-*p23Δ158-209*(T36)-, 35S-*p23*(T36)-, 35S-*p23*(T317), 35S-*p23Δ158-209*(T36)-, empty vector (EV)-transgenic limes and non-transgenic limes infected with CTV T36 (C+CTV), stained with a combination of safranin O and Fast Green FCI. (a, i) Healthy leaves from non-inoculated 6 and 12 month-old EV transgenic plants, respectively. (b) Vein clearing area from a non-transgenic lime infected with CTV T36 (C+CTV). (c-e) Vein clearing area from 35S-*p23*(T36)- (c), 35S-*p23*(T317)- (d) and 35S-*p23Δ158-209*(T36)- (e) transgenic plants. (f-h) Vein clearing area from CoYMV-*p23*(T36)- (f), CoYMV-*p23*(T317)- (g) and CoYMV-*p23Δ158-209*(T36)- (h) transgenic plants. (j) Vein corking area from a non-transgenic lime infected with CTV T36 (C+CTV). (k) Necrotic vein from a CoYMV-*p23*(T36)-transgenic plant. (l) Necrotic vein from a CoYMV-*p23Δ158-209*(T36)-transgenic plant. The white rectangles in (a) to (l) are shown at higher magnification in adjacent panels indicated by black arrows. Symbols: (X) xylem; (P) phloem; (P.f.) phloem fiber; (H) hypertrophic cells; obliterated cells, collapsed areas, and necrotic areas are indicated by small red, yellow, and long red arrows, respectively.

How phloem-specific expression of p23 incites CTV-like symptoms in Mexican lime?

Transgenic expression of p23 in Mexican lime controlled by a phloem-specific promoter mimics virus-induced symptoms more accurately than when expressed from a constitutive promoter. Particularly, phloem-specific expression of p23(T36) and p23Δ158-209(T36) in Mexican lime induced, in addition to vein clearing, vein necrosis and stem pitting very similar to those induced by T36 in non-transformed plants. Similarly, phloem-specific expression of p23(T317) induced vein clearing but not vein necrosis or stem pitting, recapitulating symptoms incited by T317 in non-transformed plants. In contrast, constitutive expression of p23 (from T36 or T317) failed to induce vein necrosis, but resulted in chlorotic pinpoints, apical necrosis and mature leaf epinasty (not observed in natural CTV infections) (Fagoaga et al., 2005; Ghorbel et al., 2001). Therefore, these latter aberrations are most likely associated to the ectopic accumulation of this protein in non-phloem cells, wherein CTV does not replicate and accumulate.

We have previously suggested that it is unlikely that p23 might interfere with synthesis of virus-derived small RNAs (vsRNAs) because they accumulate at very high levels in Mexican lime and some other CTV-infected citrus hosts (Fagoaga et al., 2006; Ruiz-Ruiz et al., 2011; Ruiz-Ruiz et al., 2013), with those derived from the *p23* ORF being the most abundant (Ruiz-Ruiz et al., 2011), and because accumulation of small RNAs derived from *p23* transgenes in different

configurations is insufficient to confer full resistance against CTV challenge in Mexican lime (López et al., 2010; Soler et al., 2012). p23 has characteristics in common with other viral proteins like 2b from cucumoviruses and P0 from poleroviruses, which are pathogenicity determinants that incite developmental aberrations when expressed in transgenic plants (Bortolamiol et al., 2007; Ghorbel et al., 2001; Lewsey et al., 2007; Ruiz-Ruiz et al., 2013; this work), show nuclear/nucleolar localization (Fusaro et al., 2012; González et al., 2010; Ruiz-Ruiz et al., 2013), and function as RNA silencing suppressors in *Nicotiana spp*. (Lu et al., 2004; Ruiz-Ruiz et al., 2013; Voinnet et al., 1999). Like 2b and P0, p23 might cause symptoms by targeting ARGONAUTE (AGO) proteins for degradation (Bortolamiol et al., 2007), by preventing *de novo* assembly of the RNA-induced silencing complex (RISC) (Baumberger et al., 2007; Duan et al., 2012; Zhang et al., 2006), or by promoting host epigenetic modifications via the transport of small RNA to the nucleus (Kanazawa et al., 2011). Since the region comprising the N-terminal 157 amino acids of p23 is responsible (at least in part) for symptoms in Mexican lime and, since p23Δ158-209 lacks the ability of RSS in *N. benthamiana* (Ruiz-Ruiz et al., 2013), the pathogenicity of p23 seems independent of its RSS activity (although the situation may not be the same when p23 is expressed in its natural virus-host context), and possibly linked to its subcellular localization (as well as that of p23Δ158-209) in the nucleolus and/or plasmodesmata (Ruiz-Ruiz et al., 2013). Alternatively, p23 might interact with host factors unrelated to RNA silencing pathways, as illustrated by the interactions of the

replicase protein from *Tobacco mosaic virus* with the Aux/IAA protein PAP1/IAA26 (Padmanabhan et al., 2005), the CMV 2b with catalase 3 (Inaba et al., 2011), and the p12 from a carlavirus with the promotor of a transcription factor that causes hyperplasia (Lukhovitskaya et al., 2013).

3.3.3. Experimental procedures

Recombinant vectors

The CoYMV promoter and the binary vector pGPTV harboring the CoYMV promoter were kindly provided by Dr. Neil Olszewski (University of Minnesota, USA) and Dr. Biao Ding (Ohio State University, Columbus, Ohio, USA), respectively. The DNA fragment containing the CoYMV promoter and the *nopaline synthase* terminator was excised with *Sal*I and *Eco*RI from plasmid pGPTV and then inserted into the respective restriction sites of plasmid pTZ57R (Fermentas GmbH, St. Leon-Rot, Germany) to generate the intermediate plasmid pTZ57R-CoYMV. PCR amplification of the *p23* gene from CTV-T36 (or a deletion mutant thereof) and CTV-T317 from the respective pMOG-*p23*-T36 (Ghorbel et al., 2001), pMOG-*p23Δ158-209*(T36) (Ruiz-Ruiz et al., 2013) and pMOG-*p23*-T317 (Fagoaga et al., 2005) plasmids was performed with *Pfu* DNA polymerase (Stratagene, La Jolla, CA, USA) using the sense and antisense primers RF-167 (5´-CTTggatccATGGATAATACTAGCGG-3´) and RF-168 (5´-CTTggatccTCAGATGAAGTGGTGTTC-3´), respectively, containing

a *Bam*HI restriction site (in lowercase letters) to facilitate cloning. The pMOG-*p23*-T36 plasmid was also used to generate the deletion mutant pMOG-*p23Δ158-209*(T36), in which the nucleotide guanine at position 472 was replaced by a thymine, resulting in a stop codon immediately after amino acid 157 (thus deleting the C-terminal 51 amino acids from p23 without affecting the zinc finger or any of the three flanking basic motifs). For this purpose, the pMOG-*p2*3-T36 plasmid was PCR-amplified with *Pfu* DNA polymerase using the pair of divergent primers of opposite polarity RF-353 (5'-CATCGGGTGTCTACGAGCCAGTC-3') and RF-354 (5'-CGTTCTCCGtAAGAAACTCCGG-3'), in which the lowercase letter indicates nucleotide substitution, to yield pMOG-*p23Δ158-209*(T36).

After *Bam*HI digestion, the PCR-amplified fragments were inserted between the CoYMV promoter and the *nopaline synthase* terminator (*nos*-ter) by ligation in *Bam*HI-digested pTZ57R-CoYMV plasmid, generating the intermediate plasmids pTZ57R-CoYMV-*p23*(T36); pTZ57R-CoYMV-*p23*(T317) and pTZ57R-CoYMV-*p23Δ158-209*(T36). *Eco*RI restriction sites were inserted at the 5' end of the CoYMV promoter and at the 3' end of the *nos*-ter, in the three constructions by PCR amplification using primers Phloem-D-Eco (5'-CTTgaattcGGTATCGATTTCTTAGGGGC-3') and Phloem-R-Eco (5'- CTTgaattcCCGATCTAGTAACATAGATG-3'), with the restriction site indicated in lowercase letters. The CoYMV-*p23* cassettes were digested with *Eco*RI and inserted into the unique *Eco*RI site of the binary vector pBin19-*sgfp* (Chiu et al., 1996), adjacent to the *nos*-pro/*nptII*/*nos*-ter and 35S-pro/*sgfp*/*nos*-ter cassettes (Figure

1a). The plasmid pBin19-s*gfp* was used as empty vector (EV) control. Construction of pBin19-35S-*p23*(T36), pBin19-35S-*p23*(T317) and pBin19-35S-*p23Δ158-209*(T36), with the *p23* transgenes controlled by the 35S promoter of the *Cauliflower mosaic virus* (CaMV), have been described in Ghorbel et al. (2001), Fagoaga et al. (2005) and Ruiz-Ruiz et al. (2013), respectively. Binary vectors were electroporated into the disarmed *Agrobacterium tumefaciens* strain EHA105, which was used to transform Mexican lime, as described previously (Ghorbel et al., 2001).

Transgenic plant generation

Selection of transformants was performed on a culture medium containing kanamycin (100 mg/L) and the regenerated shoots were examined under a Leica MZ 16 Stereomicroscope equipped with a GFP-Plus Fluorescence module (Leica Microsystems, Wetzlar, Germany). Shoots exhibiting bright green fluorescence were excised and grafted *in vitro* on Troyer citrange (*C. sinensis* (L.) Osb. × *Poncirus trifoliata* (L.) Raf.) seedlings (Peña and Navarro, 1999). The integrity of the *p23* transgenes was assessed by PCR with appropriate primers. PCR-positive plantlets were grafted on vigorous 6-month-old Carrizo citrange seedlings and grown in a greenhouse at 24–26ºC/ 16–18ºC (day/night), 60%–80% relative humidity and natural light. Buds from transgenic Mexican lime lines harboring the EV, the CoYMV-*p23* or the CaMV 35S-*p23* cassettes (Ghorbel et al., 2001; Fagoaga et al., 2005; Ruiz-Ruiz et al, 2013), or from non-transgenic control plants

infected with CTV T36 or CTV T317 were propagated on vigorous Carrizo citrange rootstocks in parallel. Plants were grown in individual 2.5 L pots containing a mixture of 55% Sphagnum peat and 45% siliceous sand, and were fertilized weekly.

The growth and symptom expression of transgenic and non-transgenic CTV-infected Mexican lime plants was periodically observed for at least three years. Developmental aberrations in transgenic lines and CTV-induced symptoms in infected plants were photographed with a Nikon D80 camera, and specific details from leaves and peeled branches were photographed with a Leica MZ 16 Stereomicroscope equipped with a camera Leica DFC490 (Leica Microsystems).

Southern, Northern and Western blot analyses

To analyze the integrity and loci number of the CoYMV-*p23* expression cassettes in Mexican lime plants, Southern blot hybridization analysis was performed. DNA aliquots (15 μg) extracted from leaves (Dellaporta et al., 1983) were digested with *Eco* RI, which excises the expression cassettes (Figure 1a), or with *Nhe* I, which cuts once the T-DNA (Figure 1a). After agarose gel electrophoresis, the DNA was blotted on to positively charged nylon membranes, fixed by UV irradiation, probed with a digoxigenin (DIG)-labelled cDNA fragment of the *p23* coding region prepared by PCR according to the manufacturer's instructions (Boehringer Mannheim GmbH, Mannheim, Germany) and detected using the chemiluminescent CSPD

substrate (Roche, Diagnostics Corporation, Indianapolis, USA). For detection of transgene-derived transcripts, Northern blot hybridization analysis was perfomed. Total RNA from leaf midribs of the transgenic plants was extracted with buffer-saturated phenol and fractionated with 2 M LiCl (Carpenter and Simon, 1998). Aliquots (20 μg) of the insoluble RNA fraction were electrophoresed in 1% agarose gels containing formaldehyde, blotted on to nylon membranes, fixed by UV irradiation and probed with a digoxigenin-labelled cDNA fragment of the *p23* coding region, according to the manufacturer's instructions (Boehringer-Mannheim) and detected by chemiluminescence with the CSPD substrate (Roche).

The accumulation of p23 and p23Δ158-209 proteins in the transgenic Mexican lime plants was tested by Western blot analysis. Total protein was extracted from leaf midribs with 100 mM Tris-HCl, pH 6.8, containing 0.3% β-mercaptoethanol and 1 mM phenyl-methyl-sulfonyl fluoride, and quantified with the Protein Assay Dye Reagent (Bio-Rad, Hercules, CA, USA) using bovine serum albumin as standard (Bradford, 1976). Aliquots (50 μg) were electrophoresed in SDS-polyacrylamide gels (12%), electroblotted onto PVDF membranes, and probed with a polyclonal antibody (1 μg/ml) against p23Δ50-86 (Ruiz-Ruiz et al., 2013). Binding of the antibody was detected with goat anti-rabbit IgG conjugated with alkaline phosphatase (Sigma-Aldrich, St Louis, MO, USA) and visualized with 5-Bromo-4-chloro-3-indolyl phosphate/Nitro blue tetrazolium SIGMA *FAST*™ BCIP/NBT (Sigma-Aldrich). Extracts from leaf midribs of

transgenic Mexican lime plants carrying the EV control construct and from non-transgenic Mexican limes infected with CTV (C+CTV) were used as negative and positive controls, respectively.

Histological analysis

Leaf pieces of approximately 1 x 0.5 cm, including minor veins and midribs, were collected from areas with vein clearing or vein necrosis aberrations from CoYMV-*p23*(T36)-, CoYMV-*p23Δ158-209*(T36)-, and CoYMV-*p23*(T317)-transgenic Mexican lime plants, from their 35S-*p23* counterparts, from symptomatic areas of non-transgenic CTV-infected Mexican limes, and from similar asymptomatic areas of non-infected EV control plants.

Leaf samples were fixed in FAA solution (0.5:9:0.5, vol/vol/vol of formaldehyde, ethanol, acetic acid) for 15 days and dehydrated through a series of ethanol/ tertiary butyl alcohol solutions (Jensen, 1962). After embedding them in histosec® pastilles (solidification point: 56 to 58°C) (Merck, One Merck Drive, Whitehouse Station, NJ, USA), ten micrometer thick cross sections of leaf veins were obtained with a rotary microtome (Jung, Heidelberg, Germany). Sections were stained with a combination of safranin O (Merck) (lignified cellular walls stain red) and Fast Green FCI (Sigma- Aldrich) (cellulose stains blue-green), mounted with Canada balsam (Merck) (Jensen, 1962; Román et al., 2004), and examined and photographed with a Leica DMLS microscope equipped with a Leica DFC490 digital camera.

Acknowledgements

We thank J.E. Peris, J. Juárez and M.T. Gorris for their excellent technical assistance. N.S. was supported by a PhD fellowship from the IVIA. This research was supported by grants AGL2009-08052, co-financed by Fondo Europeo de Desarrollo Regional-MICINN, and Prometeo ⁄ 2008 ⁄ 121 from the Generalitat Valenciana.

References

Albiach-Martí, M.R., Robertson, C., Gowda, S., Tatineni, S., Belliure, B., Garnsey, S.M., Folimonova, S.Y., Moreno, P. and Dawson, W.O. (2010) The pathogenicity determinant of *Citrus tristeza virus* causing the seedling yellows syndrome maps at the 3'-terminal region of the viral genome. *Mol. Plant Pathol*. **11**, 55-67.

Bar-Joseph, M., Marcus, R. and Lee, R.F. (1989) The continuous challenge of *Citrus tristeza virus* control. *Annu. Rev. Phytopathol*. **27**, 291-316.

Baumberger, N., Tsai, C.H., Lie, M., Havecker, E. and Baulcombe, D.C (2007) The Polerovirus silencing suppressor P0 targets ARGONAUTE proteins for degradation. *Curr. Biol.* **17**, 1609-1614.

Bortolamiol, D., Pazhouhandeh, M., Marrocco, K., Genschik, P. and Ziegler-Graff, V. (2007) The Polerovirus F box protein P0 targets ARGONAUTE1 to suppress RNA silencing. *Curr. Biol.* **17**, 1615-1621.

Bradford, M.M. (1976) A rapid and sensitive method for the quantitation of microgram quantities of protein utilizing the principle of protein-dye binding. *Anal. Biochem*. **72**, 248-254.

Carpenter, C.D. and Simon, A.E. (1998) Preparation of RNA. *Methods Mol. Biol*. **82**, 85-89.

Chiu, W., Niwa, Y., Zeng, W., Hirano, T., Kobayashi, H. and Sheen, J. (1996) Engineered GFP as a vital reporter in plants. *Curr. Biol*. **6**, 325-330.

Csorba, T., Pantaleo, V. and Burgyan, J. (2009) RNA silencing: An antiviral mechanism. *Adv. Virus Res*. **75**, 35-71.

Dellaporta, S.L., Wood, J. and Hicks, J.B. (1983) A plant DNA minipreparation: Version II. *Plant Mol. Biol. Rep.* **1**, 19-21.

Díaz-Pendón, J.A. and Ding, S.W. (2008) Direct and indirect roles of viral suppressors of RNA silencing in pathogenesis. *Annu. Rev. Phytopathol*. **46**, 303-326.

Dolja, V.V., Karasev, A.V. and Koonin, E.V. (1994) Molecular-biology and evolution of closteroviruses - sophisticated buildup of large RNA genomes. *Annu. Rev. Phytopathol.* **32**, 261-285.

Dolja, V.V., Kreuze, J.F. and Valkonen, J.P. (2006) Comparative and functional genomics of closteroviruses. *Virus Res*. **117**, 38-51.

Duan, C.G., Fang, Y.Y., Zhou, B.J., Zhao, J.H., Hou, W.N., Zhu, H., Ding, S.W. and Guo, H.S. (2012) Suppression of Arabidopsis ARGONAUTE1-mediated slicing, transgene-induced RNA silencing, and DNA methylation by distinct domains of the *Cucumber mosaic virus* 2b protein. *Plant Cell,* **24**, 259-274.

Fagoaga, C., López, C., Hermoso de Mendoza, A., Moreno, P., Navarro, L., Flores, R. and Peña, L. (2006) Post-transcriptional gene silencing of the p23 silencing suppressor of *Citrus tristeza virus* confers resistance to the virus in transgenic Mexican lime. *Plant Mol. Biol*. **60**, 153-165.

Fagoaga, C., López, C., Moreno, P., Navarro, L., Flores, R. and Peña, L. (2005) Viral-like symptoms induced by the ectopic expression of the *p23* gene of *Citrus tristeza virus* are citrus specific and do not correlate with the pathogenicity of the virus strain. *Mol. Plant Microbe Interact.* **18**, 435-445.

Fagoaga, C., Pensabene-Bellavia, G., Moreno, P., Navarro, L., Flores, R. and Peña, L. (2011) Ectopic expression of the p23 silencing suppressor of *Citrus tristeza virus* differentially modifies viral accumulation and tropism in two transgenic woody hosts. *Mol. Plant Pathol*. **12**, 898-910.

Febres, V., Ashoulin, L., Mawassi, M., Frank, A., Bar-Joseph, M., Manjunath, K., Lee, R. and Niblett, C. (1996) The p27 protein is present at one end of *Citrus tristeza virus* particles. *Phytopathology*, **86**, 1331.

Folimonova, S.Y. (2012) Superinfection exclusion is an active virus-controlled function that requires a specific viral protein. *J. Virol.* **86**, 5554-5561.

Fusaro, A.F., Correa, R.L., Nakasugi, K., Jackson, C., Kawchuk, L., Vaslin, M.F. and Waterhouse, P.M. (2012) The Enamovirus P0 protein is a silencing suppressor which inhibits local and systemic RNA silencing through AGO1 degradation. *Virology*, **426**, 178-187.

Ghorbel, R., López, C., Fagoaga, C., Moreno, P., Navarro, L., Flores, R. and Peña, L. (2001) Transgenic citrus plants expressing the *Citrus tristeza virus* p23 protein exhibit viral-like symptoms. *Mol. Plant Pathol.* **2**, 27-36.

González, I., Martínez, L., Rakitina, D.V., Lewsey, M.G., Atencio, F.A., Llave, C., Kalinina, N.O., Carr, J.P., Palukaitis, P. and Canto, T. (2010) *Cucumber mosaic virus* 2b protein subcellular targets and interactions: their significance to RNA silencing suppressor activity. *Mol. Plant Microbe Interact.* **23**, 294-303.

Gowda, S., Satyanarayana, T., Davis, C.L., Navas-Castillo, J., Albiach-Martí, M.R., Mawassi, M., Valkov, N., Bar-Joseph, M., Moreno, P. and Dawson, W.O. (2000) The *p20* gene product of *Citrus tristeza virus* accumulates in the amorphous inclusion bodies. *Virology*, **274**, 246-254.

Hilf, M.E., Karasev, A.V., Pappu, H.R., Gumpf, D.J., Niblett, C.L. and Garnsey, S.M. (1995) Characterization of *Citrus tristeza virus* subgenomic RNAs in infected tissue. *Virology*, **208**, 576-582.

Hsieh, Y.C., Omarov, R.T. and Scholthof, H.B. (2009) Diverse and newly recognized effects associated with short interfering RNA binding site modifications on the *Tomato bushy stunt virus* p19 silencing suppressor. *J. Virol.* **83**, 2188-2200.

Inaba, J., Kim, B.M., Shimura, H. and Masuta, C. (2011) Virus-induced necrosis is a consequence of direct protein-protein interaction between a viral RNA-silencing suppressor and a host catalase. *Plant Physiol.* **156**, 2026-2036.

Jensen, W.A. (1962) Botanical Histochemistry: Principles and Practice. San Francisco: W.H. Freeman.

Kanazawa, A., Inaba, J., Shimura, H., Otagaki, S., Tsukahara, S., Matsuzawa, A., Kim, B. M., Goto, K. and Masuta, C. (2011) Virus-mediated efficient induction of epigenetic modifications of endogenous genes with phenotypic changes in plants. *Plant J.* **65**, 156-168.

Karasev, A.V., Boyko, V.P., Gowda, S., Nikolaeva, O.V., Hilf, M.E., Koonin, E.V., Niblett, C.L., Cline, K., Gumpf, D.J. and Lee, R.F. (1995) Complete sequence of the *Citrus tristeza virus* RNA genome. *Virology,* **208**, 511-520.

Lewsey, M., Robertson, F.C., Canto, T., Palukaitis, P. and Carr, J.P. (2007) Selective targeting of miRNA-regulated plant development by a viral counter-silencing protein. *Plant J.* **50**, 240-252.

López, C., Ayllon, M.A., Navas-Castillo, J., Guerri, J., Moreno, P. and Flores, R. (1998) Molecular variability of the 5'- and 3'-terminal regions of *Citrus tristeza virus* RNA. *Phytopathology,* **88**, 685-691.

López, C., Cervera, M., Fagoaga, C., Moreno, P., Navarro, L., Flores, R. and Peña, L. (2010) Accumulation of transgene-derived siRNAs is not sufficient for RNAi-mediated protection against *Citrus tristeza virus* in transgenic Mexican lime. *Mol. Plant Pathol.* **11**, 33-41.

López, C., Navas-Castillo, J., Gowda, S., Moreno, P. and Flores, R. (2000) The 23-kDa protein coded by the 3'-terminal gene of *Citrus tristeza virus* is an RNA-binding protein. *Virology,* **269**, 462-470.

Lu, R., Folimonov, A., Shintaku, M., Li, W.X., Falk, B.W., Dawson, W.O. and Ding, S.W. (2004) Three distinct suppressors of RNA silencing encoded by a 20-kb viral RNA genome. *Proc. Natl. Acad. Sci. USA,* **101**, 15742-15747.

Lukhovitskaya, N.I., Solovieva, A.D., Boddeti, S.K., Thaduri, S., Solovyev, A.G. and Savenkov, E.I. (2013) An RNA virus-encoded zinc-finger protein acts as a plant transcription factor and induces a regulator of cell size and proliferation in two tobacco species. *Plant Cell,* **25**, 960-973.

Medberry, S.L., Lockhart, B.E. and Olszewski, N.E. (1992) The *commelina yellow mottle virus* promoter is a strong promoter in vascular and reproductive tissues. *Plant Cell,* **4**, 185-192.

Moreno, P., Ambrós, S., Albiach-Martí, M.R., Guerri, J. and Peña, L. (2008) *Citrus tristeza virus*: A pathogen that changed the course of the citrus industry. *Mol. Plant Pathol*. **9**, 251-268.

Moreno, P., Guerri, J., Ballester-Olmos, J.F., Albiach-Martí, M.R. and Martínez, M.E. (1993) Separation and interference of strains from a *Citrus tristeza virus* isolate evidenced by biological activity and double-stranded RNA (dsRNA) analysis. *Plant Pathol.* **42**, 35-41.

Navas-Castillo, J., Albiach-Martí, M.R., Gowda, S., Hilf, M.E., Garnsey, S.M. and Dawson, W.O. (1997) Kinetics of accumulation of *Citrus tristeza virus* RNAs. *Virology*, **228**, 92-97.

Padmanabhan, M.S., Goregaoker, S.P., Golem, S., Shiferaw, H. and Culver, J.N. (2005) Interaction of the *Tobacco mosaic virus* replicase protein with the Aux/IAA protein PAP1/IAA26 is associated with disease development. *J. Virol.* **79**, 2549-2558.

Pappu, H.R., Karasev, A.V., Anderson, E.J., Pappu, S.S., Hilf, M.E., Febres, V.J., Eckloff, R.M., McCaffery, M., Boyko, V. and Gowda, S. (1994) Nucleotide sequence and organization of eight 3' open reading frames of the Citrus tristeza closterovirus genome. *Virology*, **199**, 35-46.

Pappu, S.S., Febres, V.J., Pappu, H.R., Lee, R.F. and Niblett, C.L. (1997) Characterization of the 3' proximal gene of the Citrus tristeza closterovirus genome. *Virus Res*. **47**, 51-57.

Peña, L. and Navarro, L. (1999) Transgenic citrus. In *Biotechnology in Agriculture and Forestry*, Vol. **44**, *Transgenic Trees* (Y.P.S. Bajaj, ed.). Berlin/Heidelberg: Springer-Verlag, pp. 39-54.

Román, M.P., Cambra, M., Juárez, J., Moreno, P., Duran-Vila, N., Tanaka, F.A.O., Alves, E., Kitajima, E.W., Yamamoto, P.T., Bassanezi, R.B., Teixeira, D.C., Jesus Junior, W.C., Ayres, A.J., Gimenes-Fernandes, N., Rabenstein, F., Girotto, L.F. and Bové, J.M. (2004) Sudden death of citrus in Brazil: A graft-transmissible bud union disease. *Plant Dis.* **88**, 453-467.

Ruiz-Ruiz, S., Navarro, B., Gisel, A., Peña, L., Navarro, L., Moreno, P., Di Serio, F. and Flores, R. (2011) *Citrus tristeza virus* infection induces the accumulation of viral small RNAs (21-24-nt) mapping preferentially at the 3'-terminal region of the genomic RNA and affects the host small RNA profile. *Plant Mol. Biol.* **75**, 607-619.

Ruiz-Ruiz, S., Soler, N., Sánchez-Navarro, J., Fagoaga, C., López, C., Navarro, L., Moreno, P., Peña, L. and Flores, R. (2013) *Citrus tristeza virus* p23: Determinants for nucleolar localization and their influence on suppression of RNA silencing and pathogenesis. *Mol. Plant Microbe Interact.* **26**, 306-318.

Sambade, A., López, C., Rubio, L., Flores, R., Guerri, J. and Moreno, P. (2003) Polymorphism of a specific region in gene *p23* of *Citrus tristeza virus* allows discrimination between mild and severe isolates. *Arch. Virol.* **148**, 2325-2340.

Satyanarayana, T., Gowda, S., Ayllon, M.A., Albiach-Martí, M.R., Rabindran, S. and Dawson, W.O. (2002) The p23 protein of *Citrus tristeza virus* controls asymmetrical RNA accumulation. *J. Virol.* **76**, 473-483.

Satyanarayana, T., Gowda, S., Ayllon, M.A. and Dawson, W.O. (2004) Closterovirus bipolar virion: Evidence for initiation of assembly by minor coat protein and its restriction to the genomic RNA 5' region. *Proc. Natl. Acad. Sci. USA*, **101**, 799-804.

Satyanarayana, T., Gowda, S., Boyko, V.P., Albiach-Martí, M.R., Mawassi, M., Navas-Castillo, J., Karasev, A.V., Dolja, V., Hilf, M.E., Lewandowski, D.J., Moreno, P., Bar-Joseph, M., Garnsey, S.M. and Dawson, W.O. (1999) An engineered closterovirus RNA replicon and analysis of heterologous terminal sequences for replication. *Proc. Natl. Acad. Sci. USA*, **96**, 7433-7438.

Satyanarayana, T., Gowda, S., Mawassi, M., Albiach-Martí, M.R., Ayllon, M.A., Robertson, C., Garnsey, S.M. and Dawson, W.O. (2000) Closterovirus encoded HSP70 homolog and p61 in addition to both coat proteins function in efficient virion assembly. *Virology*, **278**, 253-265.

Schneider, H. (1959) The anatomy of tristeza-virus-infected citrus. In *Citrus Virus Diseases* (Wallace, J. M., ed.), pp. 73-84. Univ. Calif. Division Agricultural Sciences, Berkeley, CA.

Soler, N., Plomer, M., Fagoaga, C., Moreno, P., Navarro, L., Flores, R. and Peña, L. (2012) Transformation of Mexican lime with an intron-hairpin construct expressing untranslatable versions of the genes coding for the three silencing suppressors of *Citrus tristeza virus* confers complete resistance to the virus. *Plant Biotechnol. J.* **10**, 597-608.

Tatineni, S., Robertson, C.J., Garnsey, S.M., Bar-Joseph, M., Gowda, S. and Dawson, W.O. (2008) Three genes of *Citrus tristeza virus* are dispensable for infection and movement throughout some varieties of citrus trees. *Virology*, **376**, 297-307.

Tatineni, S., Robertson, C.J., Garnsey, S.M. and Dawson, W.O. (2011) A plant virus evolved by acquiring multiple nonconserved genes to extend its host range. *Proc. Natl. Acad. Sci. USA*, **108**, 17366-17371.

Voinnet, O., Pinto, Y.M. and Baulcombe, D.C. (1999) Suppression of gene silencing: a general strategy used by diverse DNA and RNA viruses of plants. *Proc. Natl. Acad. Sci. USA*, **96**, 14147-14152.

Yambao, M.L., Yagihashi, H., Sekiguchi, H., Sekiguchi, T., Sasaki, T., Sato, M., Atsumi, G., Tacahashi, Y., Nakahara, K.S. and Uyeda, I. (2008) Point mutations in helper component protease of *Clover yellow vein virus* are associated with the attenuation of RNA-silencing suppression activity and symptom expression in broad bean. *Arch. Virol.* **153**, 105-115.

Zhang, X., Yuan, Y.R., Pei, Y., Lin, S.S., Tuschl, T., Patel, D.J. and Chua, N.H. (2006) *Cucumber mosaic virus*-encoded 2b suppressor inhibits Arabidopsis Argonaute1 cleavage activity to counter plant defense. *Genes Dev.* **20**, 3255-3268.

Ziebell, H. and Carr, J.P. (2009) Effects of dicer-like endoribonucleases 2 and 4 on infection of arabidopsis thaliana by *Cucumber mosaic virus* and a mutant virus lacking the 2b counter-defence protein gene. *J. Gen. Virol*. **90,** 2288-2292.